scientific reports

Check for updates

OPEN

Effects of phosphoric acid concentration on properties of activated carbon from *Strychnos spinose* fruit shells

John Chagu[1] & Alinanuswe Joel Mwakalesi[2]✉

The accumulation of agricultural wastes in the environment is an emerging challenge. Their thermochemical conversion to activated carbon represents an efficient form of utilization that minimizes the secondary pollution caused by conventional treatment methods, such as incineration and landfilling. This study reports the synthesis and characterization of activated carbon from an affordable, abundant, and underutilized source of *Strychnos spinosa* fruit shells. The activated carbon was prepared through chemical activation using phosphoric acid of different concentrations (30%, 60%, 100%, and 150%), followed by physical activation at 500 °C for 4 h. The influence of the activating agent concentrations on the properties of activated carbon, such as yield, moisture content, ash content and iodine number, was studied. Additionally, X-ray diffraction, scanning electron microscopy, Brunauer–Emmett–Teller and Infrared spectroscopy techniques were used to study characteristics of activated carbon. The results showed that the yield of activated carbon increased from 25.33% to 29.2% as the concentration of phosphoric acid increased from 30% to 150%. The increased acid concentration also increased the moisture content, ash content and iodine number of the activated carbon. The highest iodine number of 999 mg/g was obtained for the activated carbon with the surface area of 507.373 m²/g impregnated with 150% phosphoric acid. Similarly, the SEM images revealed larger pore sizes for activated carbon produced using 150% phosphoric acid compared to those produced using 30%, 60% and 100% phosphoric acid. The findings demonstrate that phosphoric acid concentration influences the properties and performance of the *Strychnos spinosa* fruit shell activated carbon.

Keywords Activated carbon, *Strychnos spinose*, Fruit shells, BET, Phosphoric acid

Water pollution remains a global environmental challenge, caused by increasing industrialization, urbanization, and agricultural activities. Thus, different techniques have been employed to remove chemical contaminants from water, including filtration, biological treatments, electrolysis, adsorption, and the activated sludge process[1]. Among these, the adsorption is widely regarded as one of the most effective methods for removing pollutants from both liquids and gases. The activated carbon is one of the most commonly used adsorbents due to its high porosity, large surface area, and excellent adsorption capacity[2]. However, the commercially produced activated carbons are relatively expensive because they are derived from high-cost sources such as coal, coke, petroleum, peat, and refinery residue[3]. As a result, researchers are exploring the production of activated carbon using more cost-effective alternatives.

The use of agricultural by-products for making activated carbon has emerged as a highly promising and cost-effective method because of their cheapness, environmental friendliness and renewability. The method not only addresses the environmental challenge of agro-waste disposal but also transforms these wastes into valuable adsorbents[4]. Thus, activated carbon from various agricultural wastes such as olive stones, rice husks, almond shells, sawdust, corn cobs, and waste tea is known[5]. The materials exhibit favourable physicochemical properties for activation, such as high lignocellulosic content and inherent porosity, which make them suitable for developing high-performance adsorbents. Several studies have demonstrated the development of effective

[1]Department of Natural Sciences, Mbeya University of Science and Technology, P.O. Box 131, Mbeya, Tanzania. [2]Department of Chemistry and Physics, College of Natural and Applied Sciences, Sokoine University of Agriculture, P.O. Box 3038, Morogoro, Tanzania. ✉email: mwakalesi@sua.ac.tz

activated carbons from these waste materials for the removal of chemicals like heavy metals, dyes, pesticides, and pharmaceutical residues from water[6].

Strychnos spinosa, commonly known as the spiny monkey orange, is a deciduous tree native to sub-Saharan Africa. This small to medium-sized tree, ranging from 1 to 7 m in height[7]. It is characterized by curved and straight axillary spines and a corky bark. It bears globular, edible fruits with diameters ranging from 6 to 15 cm, visually resembling typical oranges. A single mature tree is capable of yielding between 300 and 700 fruits per season, contributing a total fruit mass of approximately 40 to 100 kg[8]. During ripening, the fruit's outer peel transitions from green to yellow and is approximately 34 mm thick when unripe. The shells of *S. spinosa* fruit are typically discarded as agricultural waste. However, the shells are rich in phytochemicals, including phenylpropanoids and eugenol, which are recognized for their antimicrobial and antioxidant properties[9]. Additionally, they contain substantial amounts of lignocellulosic biomass, making them a suitable candidate for the production of activated carbon. A prior study demonstrated the successful conversion of these shells into biochar/activated carbon, which exhibited promising performance for the removal of anionic dyes from wastewater[10,11]. The use of phosphoric acid produced activated carbon with high adsorption capacity and surface area compared to zinc chloride[11]. Despite this initial exploration, there remains a research gap, as no studies have systematically investigated the potential effects of phosphoric acid concentration on properties of the activated carbon prepared from *S. spinosa* fruit shells. Therefore, the current study is an attempt to fabricate the activated carbon with a high surface area and enhanced adsorption properties from *S. spinosa* fruit shells, using varying concentrations of phosphoric acid activating agent. This study intends to establish the quality of activated carbon fabricated from the shells using different concentrations of phosphoric acid. The findings contribute to reducing agricultural waste, which can cause ecological and health problems when discarded in the environment. Phosphoric acid was chosen as an activating agent because it is an environmentally friendly and cost-effective alternative to chemicals like H_2SO_4 and KOH[12]. It also produces activated carbon with an excellent mesoporous structure characterized by high pore volume and diameter[13].

Experimental part

Materials

Ortho phosphoric acid (85%), Sulphuric acid (98%), sodium hydroxide (97%), hydrochloric acid (37%), and sodium hydrogen carbonate (99.7%) from LOBA CHEMIE PVT. LTD, Mumbai (India). *S. spinosa* fruit shells collected from Makere village in Kasulu District, Kigoma-Tanzania were used as the precursor for activated carbon.

Preparation of activated carbon

The activated carbon was prepared using the procedures previously reported[14,15]. A powdered sample of *S. spinosa* fruit shells (30 g) was soaked for 24 h in 600 mL solution of different concentrations of phosphoric acid 30% (0.1529 M), 60% (0.3061 M), 100% (0.5102 M), and 150% (0.7653 M). The mixture was filtered through a Whitman filter paper (0.7 µm) and the collected solid sample was dried in the oven at 110 °C for 36 h. The dried sample was then heated at 500 °C for 4 h in the muffle furnace. The pyrolysis conditions of 500 °C and a duration of 4 h were reported to facilitate the evaporation of little volatile matter and produce a good quality activated carbon yield with more fixed carbon[16]. The resulting activated carbon was washed thoroughly with a 20% ethanol/water solution, filtered and re-soaked again in 500 mL of 1% $NaHCO_3$ for 1 h. The resulting mixture was filtered and washed with distilled water to attain pH of 7 for each, then each filtrate was taken to the oven and dried for 24 h at 110 °C. The obtained activated carbon was stored in the glass vial for characterization.

Characterization of activated carbon

Yield

Yield reflects the mass loss of the precursor during activated carbon preparation and was determined using Eq. 1.

$$\text{Yield } (\%) = \frac{\text{mass of activated carbon}}{\text{mass of precursor}} \times 100\% \quad (1)$$

Moisture content

The moisture content was determined by using standard procedures (ASTM D1763-84). The known mass (M_0) of activated carbon was weighed and placed in an oven at 110 °C for 24 h. After its removal from the oven, the crucible containing the sample was cooled in a desiccator and reweighed to obtain a constant mass. The moisture content was calculated using Eq. 2.

$$\text{Moisture content } (\%) = \frac{\text{mass loss}}{\text{initial mass of sample}} \times 100\% \quad (2)$$

Ash content

The ash content of activated carbon was determined using the standard method (ASTM D2866-11). A mass of 1 g of activated carbon was weighed in a crucible and placed in an oven at 650 °C for 4 h. The crucible was then cooled to room temperature and weighed again. The ash content was calculated using Eq. 3.

$$\text{Ash content } (\%) = \frac{\text{mass of sample after ash process}}{\text{initial mass of sample}} \times 100\% \quad (3)$$

Iodine number

The iodine number (IN) was determined according to the standard method[17]. Briefly, 0.1 g of activated carbon synthesized with varying activating agent concentrations was mixed with 5 mL of 5% HCl. After boiling and cooling the mixture, 10 mL of 0.1 N iodine solution was added. The sample was then shaken vigorously for 30 min and titrated with a standardized 0.05 N sodium thiosulfate solution. The iodine number (IN) was calculated using Eq. 4.

$$\mathrm{IN}\left(\frac{\mathrm{mg}}{\mathrm{g}}\right) = \frac{(\mathrm{C_i} - \mathrm{C_f}) \times \mathrm{V}}{\mathrm{m}} \tag{4}$$

C_i concentration of iodine before adsorption (mol/L); C_f concentration of iodine after adsorption (mol/L); V-volume of solution (L), and m-mass of activated carbon (g).

XRD, SEM, EDX and IR

The crystalline structure of the materials was investigated by X-ray diffraction (XRD) using a Rigaku Miniflex II diffractometer. A Cu tube ($\lambda_{Cu-k\alpha}$ = 0.15418 nm, 40 kV, 30 mA) was utilized as the X-ray source. The range 10–80 (2θ°) was registered with a scan speed of 2°/min. To study the morphology, prepared activated carbons were examined by using scanning electron microscopy (SEM) (Hitachi S-4700 type II microscope), applying 10 kV acceleration voltage. Gold was applied as a conductive coating on the samples. Energy dispersive X-ray (EDX) analysis was performed using a RÖNTEC detector to identify elements and determine the chemical composition of elements in the prepared activated carbons. An IR spectrometer (Bruker Vertex 70) was used to examine the changes on the surface of activated carbon. The infrared spectra were recorded across the range 4000–400 cm^{-1} with a resolution of 4 cm^{-1}[18]. Brunauer–Emmett–Teller (BET) analysis was employed to determine the specific surface area and pore characteristics of the activated carbon.

Results and discussion

Yield

Phosphoric acid activation induces chemical transformations in biomass, such as dehydration and decomposition, that release volatile gases (e.g., CO_2, CO, H_2O, CH_4), contributing to pore formation in the resulting carbon structure[13]. To evaluate this effect, the yield of activated carbon prepared using 30%, 60%, 100% and 150% phosphoric acid concentrations was investigated. The results (Fig. 1) showed that significant mass loss occurred during the activation process. The observed mass loss is likely to be associated with the expected volatilization of oxygen and carbon atoms as gaseous by-products during pyrolysis[19]. The yield increased from 25% to 28% as the acid concentration rose from 30% to 60%, then plateaued at higher acid concentrations (60–150%). This initial increase may be attributed to the dehydration property of phosphoric acid, which stabilizes the biomass by delaying thermal decomposition, reducing volatile loss, and promoting the formation of a rigid, carbon-rich matrix[20]. However, some studies suggest that phosphoric acid facilitates the formation of a polyphosphate film on the surface of the biomass, which may help to increase the mass of activated carbon during activation[21]. Consequently, the small mass loss that occurred beyond 60% acid concentration can be a possible indicator of polyphosphate film formation in the activated carbon. Additionally, cross-linking reactions induced by phosphoric acid may contribute to the development of a stable carbon network that reduces further degradation of activated carbon[22]. A similar trend was reported for the activated carbon produced from *Myrtus communis* leaves using different phosphoric acid concentrations for the chemical activation[23]. The activated

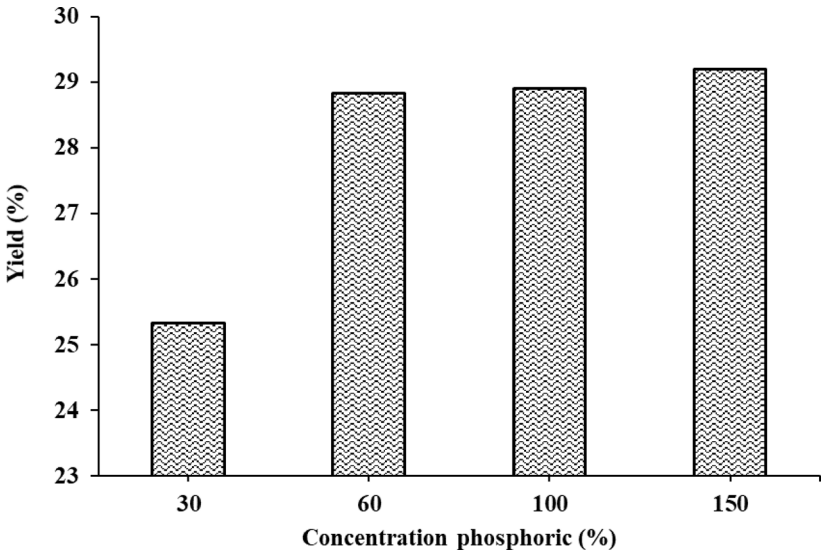

Fig. 1. Effect of phosphoric acid concentration on yield of activated carbon.

carbon produced in the current study exhibited a yield between 25 and 29%, which is closer to the established threshold value of 30%[24].

Ash content

Ash content reflects the proportion of inorganic compounds on the activated carbon, which strongly affects the adsorption capacity by altering the pore structure[25]. These inorganic residues could obstruct pores and reduce the accessible surface area for adsorption. Consequently, the activated carbon with high adsorption performance generally exhibits low ash content[26]. As shown in Fig. 2, the ash content of activated carbon increased with increasing phosphoric acid concentrations during the activation, climbing from 13% to 23% as the acid concentration was elevated from 100% to 150%. This increase may be attributed to the formation of mineral salts during pyrolysis[27]. A comparable trend has been reported in a study on activated carbon derived from *Melaleuca cajuputi* leaves, where ash content similarly increased with higher phosphoric acid concentrations[28]. The activated carbon produced using an acid concentration of 30% achieves acceptable quality, with ash content below the recommended threshold of 10%[29]. Also, the activated carbon prepared using 60% and 100% phosphoric acid produced the ash content of 13%, which is closer to the recommended value. Thus, the activated carbon prepared using 30 to 100% phosphoric acid can be of acceptable quality.

Moisture content

Moisture content refers to the water retained by activated carbon under ambient conditions. This parameter can affect adsorption performance, as water molecules may compete with target pollutants for active binding sites. As illustrated in Fig. 3, the moisture content increased with higher concentrations of phosphoric acid (the activating agent). This rise suggests that the acid treatment enhanced the material's hygroscopicity, likely due to the expansion of pore volume and surface area, which facilitates atmospheric water adsorption[23]. Despite this increase, all activated carbon samples maintained moisture levels within a narrow range of 1–6%. The limited difference in the water content is attributed to moisture adsorption from the environment post-activation, even after the high-temperature treatment that initially eliminated all water. Similar findings have been reported for coconut shell-derived activated carbon that exhibited moisture contents of 4.3–10.3%[30]. The consistently low moisture content observed indicates the suitability of the synthesized activated carbon for adsorbing chemical pollutants from the environment, as excessive moisture can compromise its performance through occupying adsorption sites[31].

Iodine number

The iodine number serves as an important indicator of activated carbon's adsorption capacity and internal surface area, reflecting its porosity, pore structure, and overall adsorption performance[32]. To assess these properties, the influence of phosphoric acid concentration on the iodine number was investigated. As shown in Fig. 4, the iodine number increased with higher phosphoric acid concentrations, rising from 660 mg/g at 30% acid concentration to 820 mg/g at 60%. The highest iodine number of 999 mg/g was achieved in the sample synthesized with 150% phosphoric acid. This enhancement is attributed to phosphoric acid's role in suppressing tar formation and facilitating the release of volatile compounds during pyrolysis, which promotes the formation of micro-pores. These micro-pores improve the adsorption efficiency of activated carbon for small-molecule adsorbates like iodine[33]. A similar iodine number of 814. 2 mg/g was previously reported for the shells prepared using phosphoric acid[11]. The results indicate that activated carbon produced with phosphoric acid concentrations between 60% and 150% exceeded the minimum iodine number threshold of 750 mg/g specified

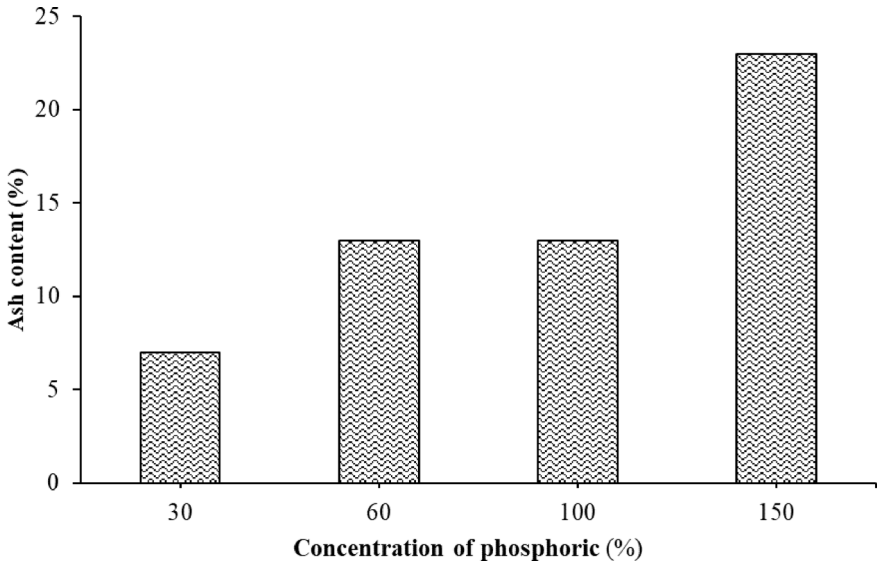

Fig. 2. Effect of concentration of phosphoric acid on yield of activated carbon.

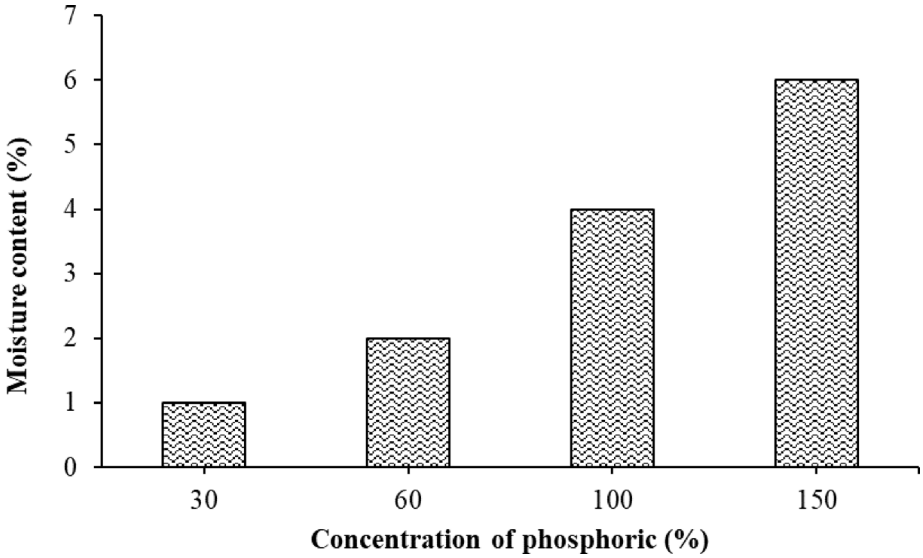

Fig. 3. Effect of concentration of phosphoric acid on yield of activated carbon.

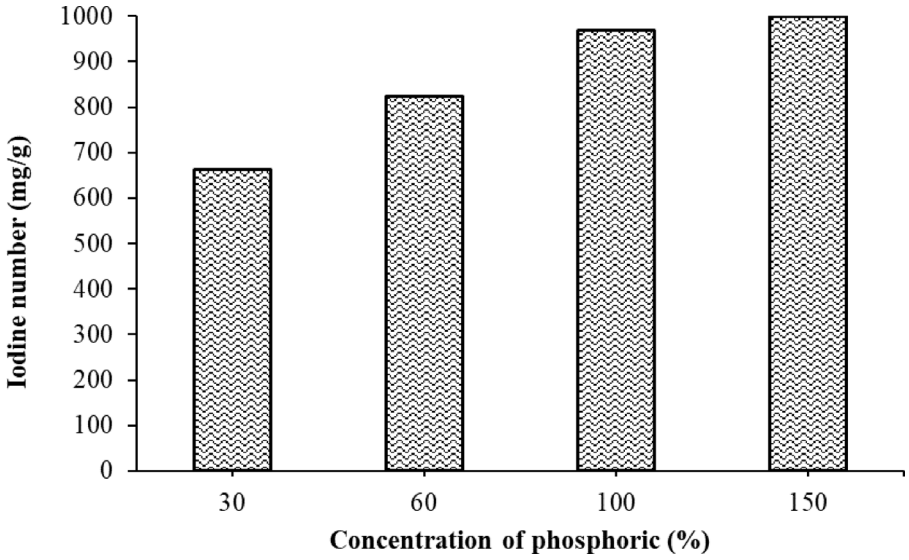

Fig. 4. Influence of phosphoric acid concentration on the iodine number.

by SNI standards (SNI-06–3730-1995)[33]. Furthermore, literature reports suggest that iodine adsorption values between 600 and 1100 mg/g are optimal for activated carbon used in water purification[24]. The iodine numbers reported in this study fall within the recommended range, confirming the suitability of the synthesized activated carbon for water purification applications.

Brunauer–emmett–teller (BET)

The effect of phosphoric acid concentration on textural characteristics such as surface area, pore surface area, pore volumes and pore radius of activated carbon is reported in Table 1. The results indicate that the BET surface area increased from 351.725 to 544.034 m^2/g as acid concentration increased from 30% to 100%. However, the decrease in the surface area from 544.034 to 507.343 m^2/g was observed at 150% phosphoric acid concentration. A similar trend was also observed for pore surface area and pore volume, which increased with the acid concentration and decreased at 150%. The observed increase in surface area and pore volume is likely due to the enhanced removal of tars from the cross-linked framework during phosphoric acid treatment[34]. The enhanced porosity can also be attributed to phosphoric acid's ability to hydrolyze cellulose, lignocellulose, and lignin in the precursor during the impregnation stage[35]. Prior studies have similarly reported increases in micro and mesopore volumes with elevated acid concentrations[36]. The findings in Table 1 further reveal an increase in pore radius as acid concentration increased, suggesting that porosity development in the activated carbon correlated with pore widening. A previous report also indicated a similar increase in pore size with higher acid concentrations[37]. This

Phosphoric acid (%)	S_{BET} (m^2/g)	S_{mes} (m^2/g)	Pore Volume (cm^3/g)	Pore Radius (Å)
30	351.725	182.130	0.275	16.847
60	288.205	192.731	0.299	16.889
100	544.034	236.762	0.356	16.655
150	507.373	216.586	0.334	16.951

Table 1. Effect of phosphoric acid concentration on specific surface area of activated carbon from *Strychnos spinose* fruit shells.

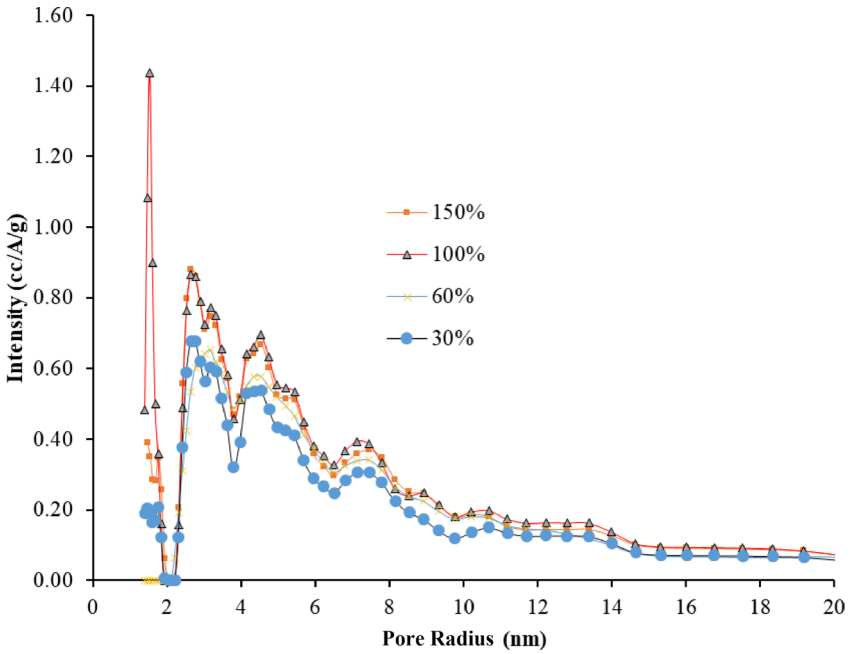

Fig. 5. Pore size distribution of activated carbon produced at different concentrations of phosphoric acid.

phenomenon was hypothesized to originate from phosphoric acid intercalated within the internal structure of lignocellulosic materials. Consequently, as acid concentration increases, the polyphosphate content within the activated carbon increases, leading to larger pore volumes[37]. However, the aggressive interaction of the high concentration of the acid with the carbon structure can cause physical collapse of the pore walls, leading to structural damage that can cause a decrease in the surface area. Thus, the observed increase in the pore radius, accompanied by the decrease in the surface area and pore volume at 150% phosphoric acid, is possible evidence of the structural damage. The decrease in the surface area and pore volume can also be associated with the adsorption of moisture as seen in Fig. 3. The adsorption can prevent adsorbate, such as nitrogen gas used for BET analysis from entering the pore network of the activated carbon due to blockage of some pores. Others also reported a similar decrease in the surface area and pore volume at higher concentrations of the acid[38,39].

Pore size distribution is an intrinsic property that influences the performance of the activated carbon and describes the structural heterogeneity of porous materials. It represents a model of the internal structure of solids, assuming that the intricate void spaces within a real material can be approximated by an equivalent set of non-interacting, uniformly shaped idealized pores[40]. In this study, the pore size distribution was determined using the Horvath-Kawazoe (HK) method[41]. The findings (Fig. 5) demonstrate that the activated carbon synthesized in this study are primarily mesoporous, with a secondary presence of microporous structures. Distinct peaks were observed across all tested impregnation ratios, indicating well-defined pore structures. As the phosphoric acid concentration increased, the formation of mesoporous and the widening of micro-pores into meso-pores became evident. However, the presence of a strong peak due to the microporous structure is observed for the activated carbon prepared using 100% phosphoric acid. This aligns with the previous results in this paper, where the activated carbon for 100% phosphoric acid showed the highest surface area. Thus, the highest surface area is likely to be attributable to the formation of a higher number of micropores in the surface of the activated carbon. A previous study has shown that the presence of micropores in carbonaceous materials is the primary contributor to their high surface area and pore volume[42].

The pore structure can also be determined through the adsorption of inert gases before liquid adsorption. The findings for N_2 adsorption–desorption isotherms at −196 °C (Fig. 6) indicated that the adsorption isotherms for activated carbon samples prepared using different impregnation ratios exhibited the type IV based on the IUPAC classification[43]. The type IV adsorption isotherm is an indicator of the mesoporous structure on the

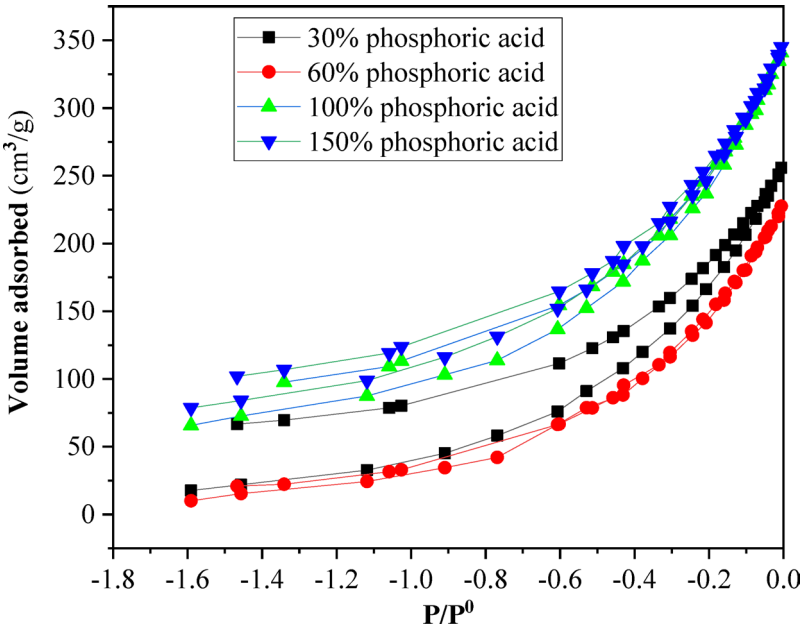

Fig. 6. N_2 adsorption isotherms for activated carbon prepared using different concentrations of phosphoric acid.

surface of the activated carbon. The observation aligns with findings that the prepared activated carbon prepared in the current study mainly contains a mixture of microporous and mesoporous materials (Fig. 5). A similar composition of microporous and mesoporous mixture of activated carbon was previously reported[44]. Although the adsorption isotherms for all activated carbons were similar, the adsorption capacities were different based on the concentration of phosphoric acid. As the concentration of phosphoric acid increases, the adsorption isotherms shift upward. A similar trend was previously reported for activated carbons prepared from olive stones using different amounts of phosphoric acid[45].

X-ray diffraction (XRD)

The XRD analysis was performed to determine the structural and compositional changes that occurred in the activated carbon samples. The results (Fig. 7) showed all the samples contained a broad peak at approximately 23° (2θ), which corresponds to (002) plane (JCPDS 41–1487) of graphitic (sp^2-bonded) carbon layers, confirming the successful preparation of activated carbons[46]. The observation agrees with previously reported XRD patterns for activated carbons prepared using desert date seed shells[47–49]. The broad nature of the peak indicates that the prepared activated carbons had an amorphous structure, highlighting the lack of long-range crystalline order within the material. The peak at around 23° (2θ) is linked to the stacking of graphene-like layers as well, with an expanded interlayer spacing compared to highly crystalline graphite. This increased spacing reflects the presence of numerous defects, functional groups, and irregularities in the graphene sheets, forming a highly disordered carbon matrix. Additionally, the findings (Fig. 7) also showed the appearance of a weak peak at around 2θ = 43°, indicating the presence of the honeycomb structures formed by sp^2-hybridized carbons[50]. The findings indicated that the structure of activated carbon prepared using different concentrations of phosphoric acid agrees with the literature as previously reported by Alouiz et al. 2024[51].

Scanning electron microscopy (SEM)

Scanning Electron Microscopy (SEM) was employed to characterize the external surface morphology of the phosphoric acid-activated carbon, specifically to evaluate the textural modifications induced by varying acid concentrations. SEM micrographs (Fig. 8) revealed that all activated carbons possessed rough surfaces with a network of irregularly shaped pores. These observable pores are a possible direct morphological consequence of the pyrolysis activation process at 500 °C[52]. During pyrolysis, phosphoric acid acts as a chemical activating agent, facilitating the decomposition and volatilization of organic compounds within the biomass precursor. The subsequent removal of these volatiles creates voids and channels, manifesting as the porous structure visible in the micrographs. The analysis of the micrographs further demonstrated a distinct correlation between phosphoric acid concentration and pore size development. The carbons activated using lower acid concentrations (30% and 60%) exhibited surfaces predominantly populated by smaller pores. In contrast, carbons produced with higher acid concentrations (100% and 150%) displayed a noticeably more developed pore structure characterized by larger pores. This trend suggests that increasing the concentration of phosphoric acid promotes more extensive volatilization of compounds of the carbon matrix, resulting in the enlargement of pore dimensions. This is a possible result of the increase in the hydrolysis of lignocellulosic material and partial extraction of components in the precursor material as the concentration of the acid increases[37]. This observed increase in pore sizes with higher acid concentration aligns directly with the iodine adsorption results reported earlier in this study (Fig.

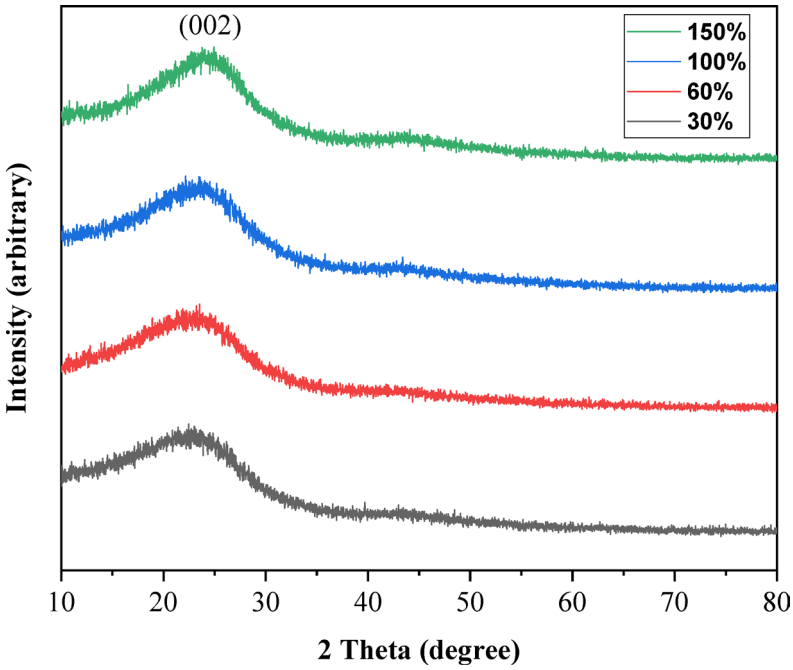

Fig. 7. XRD patterns of activated carbon prepared using different concentrations of phosphoric acid.

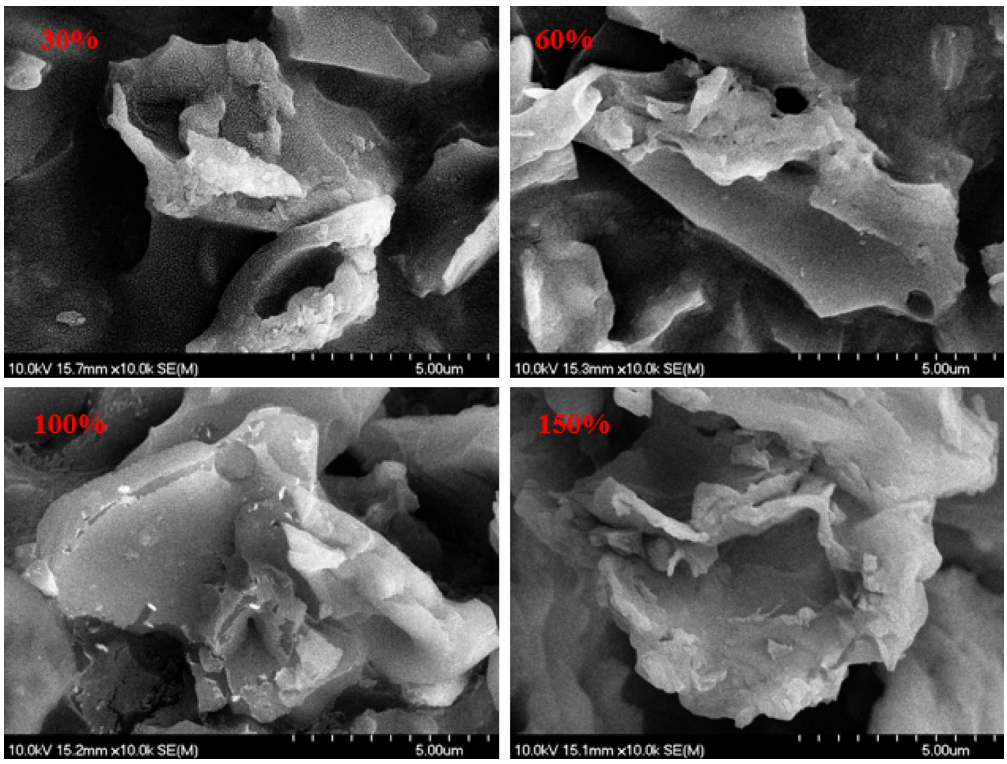

Fig. 8. SEM micrographs of activated carbon prepared using different concentrations of phosphoric acid.

4). The progressive rise in iodine number observed with increasing phosphoric acid concentration strongly correlates with the enhanced pore development observed in the SEM micrographs. The iodine adsorption is highly sensitive to the accessibility of pores within the micropore and small mesopore range. Therefore, the larger pores observed at higher acid concentrations (100% and 150%), widened entrances that facilitates greater iodine diffusion and adsorption, quantitatively confirming the morphological changes indicated by the SEM analysis.

Energy dispersive X-ray spectroscopy (EDX)

Energy Dispersive X-ray Spectroscopy (EDX) was used to quantitatively determine the elemental composition of the activated carbon samples. The EDX analysis (Fig. 9) revealed that the primary constituent was carbon, consistently ranging between 60% and 66% across all samples. Trace amounts of other mineral elements were also detected. Additionally, a clear correlation was observed between the phosphorus content and the concentration of phosphoric acid (H_3PO_4) used during the chemical activation process. The measured phosphorus contents were 0.37%, 0.77%, 0.83%, and 0.98% for activated carbon prepared using 30%, 60%, 100%, and 150% phosphoric acid, respectively. This progressive increase demonstrates that higher acid dosages lead to greater phosphorus retention within the final carbon structure. The persistence of phosphorus in the activated carbon is attributed to residual phosphoric acid and/or phosphate species that were not fully removed during the post-activation washing stage. Incomplete washing results in the incorporation of these phosphorus-containing residues into the developing porous carbon matrix during the activation process[53]. This residual phosphorus, while present at relatively low levels, likely influences the surface chemistry and adsorptive properties of the activated carbon.

Infrared spectroscopy (IR)

The results of the infrared spectroscopy (IR) analysis for the activated carbon prepared with phosphate concentrations of 30%, 60%, 100% and 150% are shown in Fig. 10. The spectra reveal that activated carbon prepared by using 30% and 150% of phosphate concentration were observed to have similar trend to certain extent in which as the wavenumber decreases from 4000 cm^{-1} to 400 cm^{-1} the transmittance (%) were increasing. For the activated carbon prepared using 60% and 100% of phosphate concentration was also observed to have their own trend which was not highly affected by the decrease in wavenumber. The IR spectra were observed to have bands at around 3750 $cm^{-1,}$ which corresponds to the COOH functional group, and at around 3415 cm^{-1} corresponds to O-H stretching[18]. The presence of COOH and O-H significantly enhances the hydrophilic properties of the activated carbon, facilitating strong hydrogen bonding interactions with polar molecules in aqueous environments[47]. The band at around 2932 cm^{-1} corresponds to C-H stretching vibrations that can be part of aliphatic chains. The bands at around 1533 cm^{-1} in all samples correspond to the C = C aromatic bond, which is more stable at a higher pyrolysis temperature[54]. The bands at around 1184 cm^{-1} were probably the stretching of the O–C bond in the P–O–C linkage (aromatic bond), which might be a result of the activation process with H_3PO_4, producing char oxidation that introduces oxygenated functionalities in the activated carbons[23,55]. The IR findings indicated that chemical activation induced surface chemistry modifications, improvements that are likely to enhance adsorption properties. Therefore, studying the interactions of the activated carbon with different chemicals can test this potential improvement.

Conclusion

The activated carbon was successfully prepared from *S. spinose* fruit shells using different concentrations of phosphoric acid. The concentration of the phosphoric acid influenced the properties of the activated carbon.

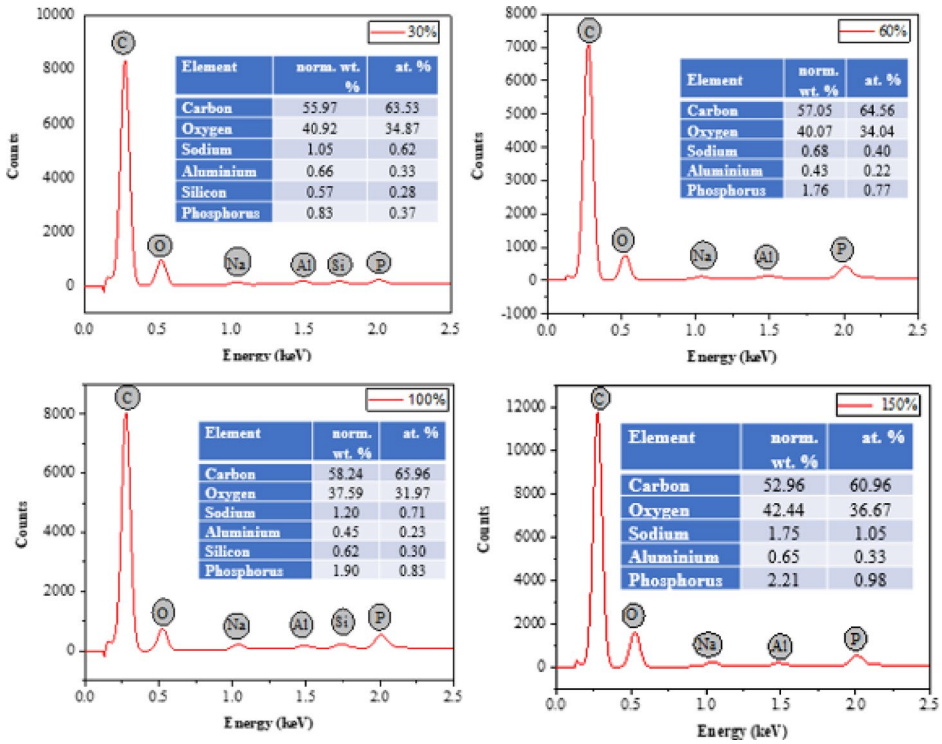

Fig. 9. EDX spectra of activated carbon prepared using different concentrations of phosphoric acid.

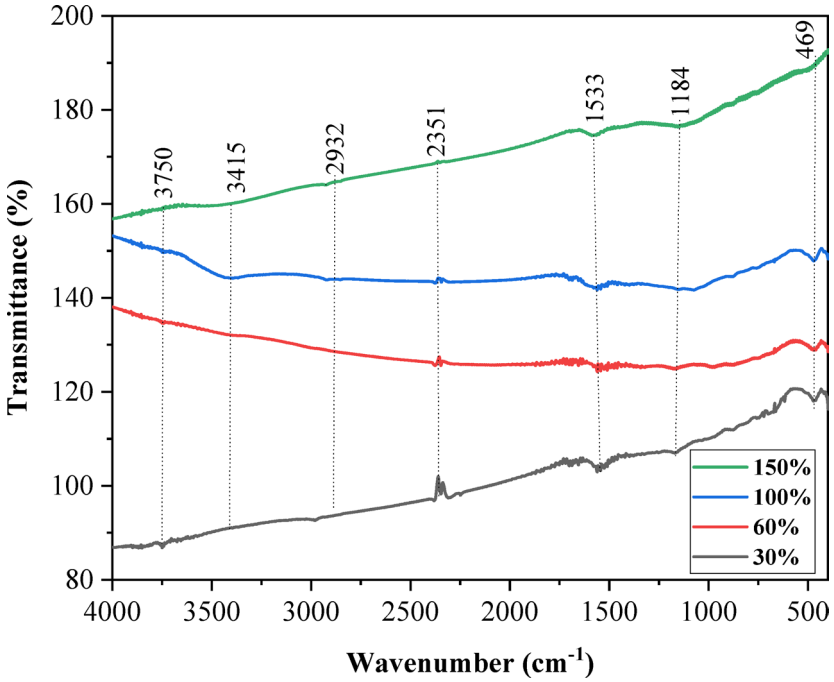

Fig. 10. IR spectra of activated carbon prepared using different concentrations of phosphoric acid.

Thus, the properties of activated carbon, such as yield, moisture content, and iodine number, increased at higher phosphoric acid concentrations. Similarly, the surface morphology of the fabricated activated carbon exhibited an increase in pore sizes as the acid concentration increased. Consequently, the surface area, pore radius and pore volume of the activated carbon increased with increasing concentration of the activating agent. However, the decrease in the surface area and pore volume was observed for activated carbon produced using 150% phosphoric acid due to the blockage of pores caused by excess phosphoric acid or its byproducts. This study confirms that *S. spinosa* fruit shells are a viable precursor for activated carbon, with a phosphoric acid concentration of 100% yielding optimal pore development and surface area, beyond which excess acid leads to pore structural degradation.

Data availability

The datasets generated during and/or analysed during the current study are available from the corresponding author on reasonable request.

Received: 27 October 2025; Accepted: 24 December 2025
Published online: 05 January 2026

References

1. Grzegorzek, M., Wartalska, K. & Kaźmierczak, B. Review of water treatment methods with a focus on energy consumption. *Int. Commun. Heat Mass Transfer.* **143**, 106674. https://doi.org/10.1016/j.icheatmasstransfer.2023.106674 (2023).
2. Kumar Mishra, R., Singh, B. & Acharya, B. A comprehensive review on activated carbon from pyrolysis of lignocellulosic biomass: An application for energy and the environment, *Carbon Resour. Convers.,* **7**(4), 100228. (2024). https://doi.org/10.1016/j.crcon.2024.100228
3. Njewa, J. B. & Shikuku, V. O. Recent advances and issues in the application of activated carbon for water treatment in africa: A systematic review (2007–2022). *Appl. Surf. Sci. Adv.* **18**, 100501. https://doi.org/10.1016/j.apsadv.2023.100501 (2023).
4. Ratan, J. K., Kaur, M. & Adiraju, B. Synthesis of activated carbon from agricultural waste using a simple method: Characterization, parametric and isotherms study, *Materials Today: Proceedings* **5**(2), Part 1 3334–3345. (2018). https://doi.org/10.1016/j.matpr.2017.11.576
5. Alslaibi, T., Abustan, I., Azmeir, M. & Foul, A. Review: Comparison of agricultural by-products activated carbon production methods using surface area response, (2012).
6. Soffian, M. S. et al. Carbon-based material derived from biomass waste for wastewater treatment. *Environ. Adv.* **9**, 100259. https://doi.org/10.1016/j.envadv.2022.100259 (2022).
7. Sitrit, Y. et al. Characterization of monkey orange (Strychnos spinosa Lam.), a potential new crop for arid regions. *J. Agric. Food Chem.* **51**, 6256–6260. https://doi.org/10.1021/jf030289e (2003).
8. Omotayo, A. O., Aremu, A. O. & Prosperity ervalued Spiny Monkey Orange (Strychnos spinosa Lam.): An Indigenous Fruit for Sustainable Food-Nutrition and Economic *Plants (Basel Switzerland)* **10**(12. https://doi.org/10.3390/plants10122785. (2021).
9. Ben-Othman, S., Jõudu, I. & Bhat, R. Bioactives from Agri-Food wastes: present insights and future challenges. *Molecules* **25**, 3. https://doi.org/10.3390/molecules25030510 (2020).
10. Obey, G., Adelaide, M. & Ramaraj, R. Biochar derived from non-customized Matamba fruit shell as an adsorbent for wastewater treatment. *J. Bioresources Bioprod.* **7** (2), 109–115. https://doi.org/10.1016/j.jobab.2021.12.001 (2022).

11. Mupa, M., Chimanikire, C., Machingauta, N. & Mukaratirwa-Muchanyereyi The efficiency of phosphoric acid and zinc chloride activated carbons prepared from strychnos spinosa fruit shell for the removal of methylene blue. *Indian J. Environ. Prot.* **38**, 896–905 (2018).
12. Carreño Hernández, G., Pulido, E., Melián, D. E. & Santiago Synthesis of activated carbon from sewage sludge using phosphoric acid as activating agent. *Environ. Sci. Pollut. Res.* https://doi.org/10.1007/s11356-025-36516-y (2025).
13. Neme, I., Gonfa, G. & Masi, C. Activated carbon from biomass precursors using phosphoric acid: A review. *Heliyon* **8** (12), e11940. https://doi.org/10.1016/j.heliyon.2022.e11940 (2022).
14. Evwierhoma, E. & Madubiko, O. A.J.N.J.o.t. Jaiyeola, Preparation and characterization of activated carbon from bean husk, **37**(3), 674–678 (2018).
15. Mpaka, L. J. & Mwakalesi, A. J. Adsorption kinetics of Picloram on chitosan-modified strychnos pungens fruit shell activated carbon. *Reaction Kinetics Mech. Catal.* https://doi.org/10.1007/s11144-025-02973-2 (2025).
16. Ashok Kumar, V. et al. Investigations on carbonization operating conditions of ANSYS customized kiln for charcoal production from prosopis Juliflora biomass and ANN model prediction for optimized operating conditions. *Fuel* **350**, 128838. https://doi.org/10.1016/j.fuel.2023.128838 (2023).
17. Mianowski, A., Owczarek, M. & Marecka, A. Surface area of activated carbon determined by the iodine adsorption number. *Energy Sources Part. A-recovery Utilization Environ. Eff.* **29**, 839–850. https://doi.org/10.1080/00908310500430901 (2007).
18. Damayanti, A. et al. Effects of Phosphate and Thermal Treatments on the Characteristics of Activated Carbon Manufactured from Durian (Durio zibethinus) Peel, *ChemEngineering* **7**(5), 75. (2023).
19. Langama, P. et al. Preparation and characterization of activated carbons from asparagus palm (Laccosperma robustum) bark by chemical activation with H_2PO_4 and KOH. *Am. J. Anal. Chem.* **14**, 55–71. https://doi.org/10.4236/ajac.2023.142004 (2023).
20. Ngouateu Lekene, R. B. et al. Preparation of activated carbons based balanites aegyptiaca shells by chemical activation: optimization conditions using the methodology of experimental design. *Eur. J. Adv. Chem. Res.* **1**, 7. https://doi.org/10.24018/ejchem.2020.1.6.33 (2020).
21. Girgis, B. S. & El-Hendawy, A. N. A. Porosity development in activated carbons obtained from date pits under chemical activation with phosphoric acid. *Microporous Mesoporous Mater.* **52**, 105–117. https://doi.org/10.1016/S1387-1811(01)00481-4 (2002).
22. Martínez-Smit, C., Chejne, F. & García-Pérez, M. Novel strategy to produce polyaromatic compounds at low temperature for the production of secondary Chars. *J. Anal. Appl. Pyrol.* **174**, 106135. https://doi.org/10.1016/j.jaap.2023.106135 (2023).
23. Megherbi, H. et al. The effect of phosphoric acid on the properties of activated carbons made from Myrtus communis leaves: textural characteristics, surface chemistry, and capacity to adsorb Methyl orange. *J. Mol. Struct.* **1321**, 140038. https://doi.org/10.1016/j.molstruc.2024.140038 (2025).
24. Divya, M. P. et al. Preparation and characterization of activated carbon from commercially important bamboo species in North Eastern India. *Adv. Bamboo Sci.* **11**, 100148. https://doi.org/10.1016/j.bamboo.2025.100148 (2025).
25. Anisuzzaman, S. M., Joseph, C. G., A.B.W. Daud, W. M., Krishnaiah, D. & Yee, H. S. Preparation and characterization of activated carbon from typha orientalis leaves. *Int. J. Industrial Chem.* **6** (1), 9–21. https://doi.org/10.1007/s40090-014-0027-3 (2015).
26. Kim, S., Lee, S. E., Baek, S. H., Choi, U. & Bae, H. J. Preparation of activated carbon from Korean anthracite: simultaneous control of Ash reduction and pore development. *Processes* **11** (10), 2877 (2023).
27. László, K., Bóta, A. & Nagyu, L. G. Characterization of activated carbons from waste materials by adsorption from aqueous solutions. *Carbon* **35** (5), 593–598. https://doi.org/10.1016/S0008-6223(97)00005-5 (1997).
28. Ibrahim, A. et al. Preparation and characterization of activated carbon obtained from melaleuca cajuputi leaves. *Carbon Trends*. **13**, 100301. https://doi.org/10.1016/j.cartre.2023.100301 (2023).
29. Zulkania, A., Hanum, G. F. & Rezki, A. S. The potential of activated carbon derived from bio-char waste of bio-oil pyrolysis as adsorbent, MATEC Web of Conferences, EDP Sciences, p. 01029. (2018).
30. Siddiqi, H., Kumari, U., Biswas, S., Mishra, A. & Meikap, B. C. A synergistic study of reaction kinetics and heat transfer with multi-component modelling approach for the pyrolysis of biomass waste. *Energy* **204**, 117933. https://doi.org/10.1016/j.energy.2020.117933 (2020).
31. Zhou, L., Li, M., Sun, Y. & Zhou, Y. J. C. Effect of moisture in microporous activated carbon on the adsorption of methane, *Carbon* **39**(5), 773–776. (2001).
32. Budianto, A., Kusdarini, E., Effendi, S. S. W. & Aziz, M. The Production of Activated Carbon from Indonesian Mangrove Charcoal, *IOP Conference Series: Materials Science and Engineering* 462(1), 012006. (2019). https://doi.org/10.1088/1757-899X/462/1/012006
33. Suliestyah, E. J. et al. Effect of phosphoric acid composition in the production and characterization of coal activated carbon, *IOP Conf. Ser.: Earth Environ. Sci.* **1422**(1), 012028. (2024). https://doi.org/10.1088/1755-1315/1422/1/012028
34. Li, Y., Zhang, X., Yang, R., Li, G. & Hu, C. The role of H3PO4 in the Preparation of activated carbon from NaOH-treated rice husk residue. *RSC Adv.* **5** (41), 32626–32636. https://doi.org/10.1039/C5RA04634C (2015).
35. Kassem, I. et al. Phosphoric acid-mediated green Preparation of regenerated cellulose spheres and their use for all-cellulose cross-linked superabsorbent hydrogels. *Int. J. Biol. Macromol.* **162**, 136–149. https://doi.org/10.1016/j.ijbiomac.2020.06.136 (2020).
36. Hsu, L. Y. & Teng, H. Influence of different chemical reagents on the Preparation of activated carbons from bituminous coal. *Fuel Process. Technol.* **64** (1), 155–166. https://doi.org/10.1016/S0378-3820(00)00071-0 (2000).
37. Molina-Sabio, M., RodRíguez-Reinoso, F., Caturla, F. & Sellés, M. J. Porosity in granular carbons activated with phosphoric acid. *Carbon* **33** (8), 1105–1113. https://doi.org/10.1016/0008-6223(95)00059-M (1995).
38. Tham, Y. J., Latif, P. A., Abdullah, A. M., Shamala-Devi, A. & Taufiq-Yap, Y. H. Performances of toluene removal by activated carbon derived from Durian shell. *Bioresour. Technol.* **102**, 724–728. https://doi.org/10.1016/j.biortech.2010.08.068 (2011).
39. Nahil, M. A. & Williams, P. T. Pore characteristics of activated carbons from the phosphoric acid chemical activation of cotton stalks. *Biomass Bioenerg.* **37**, 142–149. https://doi.org/10.1016/j.biombioe.2011.12.019 (2012).
40. Ismadji, S. & Bhatia, S. K. Characterization of activated carbons using liquid phase adsorption. *Carbon* **39** (8), 1237–1250. https://doi.org/10.1016/S0008-6223(00)00252-9 (2001). https://doi.org/https://
41. Ustinov, E. & Do, D. Adsorption in slit-like pores of activated carbons: improvement of the horvath and Kawazoe method. *Langmuir: ACS J. Surf. Colloids*. **18** (12), 4637–4647 (2002).
42. Yunes, S., Wommack, P., Still, M., Kenvin, J. & Exley, J. Physical characterization of microporous materials using various adsorbates. Correlation between their micropore volume and their capacity to adsorb H2 and CO2. *Appl. Catal. A*. **474**, 250–256. https://doi.org/10.1016/j.apcata.2013.07.049 (2014).
43. Samadi, A. et al. Standardized methodology for performance evaluation in using polyaniline-based adsorbents to remove aqueous contaminants. *J. Environ. Chem. Eng.* **12** (3), 112650. https://doi.org/10.1016/j.jece.2024.112650 (2024).
44. Park, J. E., Jo, E. S., Lee, G. B., Lee, S. E. & Hong, B. U. Adsorption capacity and desorption efficiency of activated carbon for odors from medical waste, **28**(2), 785. (2023).
45. Yakout, S. M. & Sharaf El-Deen, G. Characterization of activated carbon prepared by phosphoric acid activation of olive stones. *Arab. J. Chem.* **9**, S1155–S1162. https://doi.org/10.1016/j.arabjc.2011.12.002 (2016).
46. Yu, K., Li, J., Qi, H. & Liang, C. High-capacity activated carbon anode material for lithium-ion batteries prepared from rice husk by a facile method. *Diam. Relat. Mater.* **86**, 139–145. https://doi.org/10.1016/j.diamond.2018.04.019 (2018).
47. Elbager, M. A., Asmaly, H. A., Al-Suwaiyan, M., Ibrahim, A. I. & Dafallah, H. High performance batch adsorption of methylene blue using desert date seed shell activated carbon: characterization and response surface methodology optimization. *Water Air Soil Pollut.* **236** (4), 233. https://doi.org/10.1007/s11270-025-07880-9 (2025).

48. Thue, P. S. et al. Effects of first-row transition metals and impregnation ratios on the physicochemical properties of microwave-assisted activated carbons from wood biomass. *J. Colloid Interface Sci.* **486**, 163–175. https://doi.org/10.1016/j.jcis.2016.09.070 (2017).
49. Mamo, D. W., Asere, T. G. & Habtemariam, T. H. Adsorptive removal of Cr(VI) from aqueous solution using activated carbon of Enset root (Ensete ventricosum). *Desalination Water Treat.* **321**, 101053. https://doi.org/10.1016/j.dwt.2025.101053 (2025).
50. Caballero, A., Hernán, L. & Morales, J. Limitations of disordered carbons obtained from biomass as anodes for real Lithium-Ion batteries. *ChemSusChem* **4** (5), 658–663. https://doi.org/10.1002/cssc.201000398 (2011).
51. Alouiz, I. et al. Elaboration of fibrous structured activated carbon from Olive pomace via chemical activation and low-temperature pyrolysis. *Heliyon* **10** (20), e38886. https://doi.org/10.1016/j.heliyon.2024.e38886 (2024).
52. Ye, Y. C., Chen, W. S., Tsai, C. H. & Tsai, W. T. The combination of nitrogen (N2) pyrolysis and carbon dioxide (CO2) activation for regenerating spent activated carbon, **15**(10), 5336. (2025).
53. Guo, J. & Lua, A. C. Textural and chemical properties of adsorbent prepared from palm shell by phosphoric acid activation. *Mater. Chem. Phys.* **80** (1), 114–119. https://doi.org/10.1016/S0254-0584(02)00383-8 (2003).
54. Demiral, H. & Güngör, C. Adsorption of copper(II) from aqueous solutions on activated carbon prepared from grape Bagasse. *J. Clean. Prod.* **124**, 103–113. https://doi.org/10.1016/j.jclepro.2016.02.084 (2016).
55. Zhang, B., Wu, Y. & Cha, L. Removal of Methyl orange dye using activated Biochar derived from pomelo Peel wastes: performance, isotherm, and kinetic studies. *J. Dispers. Sci. Technol.* **41** (1), 125–136. https://doi.org/10.1080/01932691.2018.1561298 (2020).

Acknowledgements
The authors thank Mr. Liberatus Mpaka for the preparation of the plant material, and Mr. Ndabuli Mpeji and Mr. Kuchuma Mwira for their technical assistance during the experiments.

Author contributions
All authors have accepted responsibility for the entire content of this manuscript and consented to its submission to the journal, reviewed all the results and approved the final version of the manuscript. J.C and A.J.M Conceptualization, methodology, formal analysis, investigation, writing original draft preparation and editing.

Funding
The study was funded by the Sokoine University of Agriculture (SUA).

Declarations

Competing interests
The authors declare no competing interests.

Additional information
Correspondence and requests for materials should be addressed to A.J.M.

Reprints and permissions information is available at www.nature.com/reprints.

Publisher's note Springer Nature remains neutral with regard to jurisdictional claims in published maps and institutional affiliations.